

On the behaviour of urea on a heated wall - A revealed Leidenfrost-like temperature during urea thermolysis

Louis-Marie Malbec^{*1,2}, Chaouki Habchi^{1,2}, Julien Bohbot^{1,2}
Scott Drennan³, Shaoping Quan³, Dan Maciejewski³

¹IFP Energies nouvelles, 1 et 4 avenue de Bois-Préau, 92852 Rueil-Malmaison, France

²Institut Carnot IFPEN Transports Energies, 1 et 4 avenue de Bois-Préau, 92852 Rueil-Malmaison, France

³Convergent Science, Inc. - Middleton, WI 53562 - United States

*Corresponding author: louis-marie.malbec@ifpen.fr

Abstract

The interaction of single droplets with hot solid surfaces is a fundamental process for a wide range of technical applications, such as urea-water solution (UWS) injection in selective catalytic reduction (SCR) systems. Specifically, the chemical evolution and film topology and state of UWS after its deposit on a hot surface are still not well known, although these phenomena are important for the SCR efficiency.

In this work, we have experimentally and numerically investigated the behaviour of solid urea after being deposited on a heated surface. The experimental apparatus consists of a metal saucer whose surface can be heated up to 750K, on which a solid urea crystal is gently deposited. The evolution of the deposit is monitored with two cameras, showing top and side views, to record the dynamics and thermal behaviour of the urea.

The images have shown four different urea thermolysis regimes. First, urea ball melts with a melting rate increasing with wall temperature (T_w). It forms a sessile droplet at the saucer bottom that maintains its shape for a long time indicating a very small thermolysis rate. Second, at a relatively low T_w , but higher than 406K, some bubbles appear in the molten sessile droplet due to urea thermolysis gaseous products (ammonia and isocyanic acid). These bubbles nucleate at the wall, especially near the meniscus of the liquid urea lens. This phenomenon is similar to nucleate boiling of hydrocarbons liquid film. In the third stage, the urea thermolysis rate reaches a maximum critical value for T_w between 600K and 650K. Then, the images show the formation of a deposit having a very small thermolysis rate. The evolution time to reach this final state has been measured from the images. In the fourth and final stage ($T_w > 650K$), no deposit is formed on the wall and the molten urea droplet levitates and rebounds on the wall very similarly to a hydrocarbon droplet in the Leidenfrost regime. Therefore, $T_w = 650K$ may be considered as a Leidenfrost-like temperature for the urea. This temperature has been used to define the Leidenfrost regime for the urea in the map of the spray-wall interaction model. Finally, several CFD simulations have been carried in the third and fourth thermolysis stages. Thereby, the different measured evolution times have been used to check the thermolysis mechanism numerical results and to reveal the solid deposits composition that has proved to be composed of Cyanuric acid and Ammelide.

Keywords

Urea, SCR, liquid film, boiling, Leidenfrost temperature

Introduction

Urea/SCR system is currently an efficient method of NO_x control for diesel engines. In a typical SCR system, urea is typically being used as an aqueous solution at its eutectic composition (32.5% wt. urea, marketed as Adblue™). This urea-water solution (UWS) is sprayed into the hot engine exhaust upstream of the SCR catalyst. It is commonly believed that water evaporates first, often after impingement of the spray on the wall as a liquid film. The remaining urea precipitates and completely melts at wall temperature higher than 406K, then decomposes into gas phase ammonia (NH₃) and isocyanic acid (HNCO) and solid/liquid phase resulting from urea polymerization (such as biuret, cyanuric acid and ammelide). The amount and the state of these by-products depends mainly on the wall temperature. Previous studies have investigated these different processes [1–7]. However, these studies were considering UWS as the initial state. In this case, both the water evaporation and the decomposition of urea are occurring simultaneously. Especially, water evaporation potentially leads to the apparition of film boiling or Leidenfrost regime [8–11], when a vapor cushion prevents the droplet from wall wetting and therefore strongly affects thermal transfers and urea decomposition. In addition, once the water has completely evaporated, there is a need for an analysis of the decomposition of urea in the absence of water. Indeed, the thermolysis of a pure liquid urea film has not so far been studied at high wall temperature, especially during strong releases of NH₃ and HNCO. Particularly, it would be interesting and useful for CFD models to know

if the thermolysis (NH_3 and HNCO) gaseous products are able to lift the liquid urea from the wall similar to the well-known vaporous Leidenfrost effect. This study proposes an experimental and numerical analysis of the evolution of a urea crystal deposited on a heated surface. The experimental results are used to validate, in the CFD code, our previously developed urea thermolysis mechanism [1, 2]. The numerical results are in turn used to discuss the assumptions proposed on the basis of experimental results regarding the mechanisms of urea decomposition. This paper is organized as follows. Next section includes the experimental and numerical methodology. Followed by the results discussion and the conclusions.

Material and methods

Experimental methodology

The schematic diagram of the experimental apparatus used to study the thermolysis of solid urea is presented in Figure 1. A hot plate is used to heat a metallic saucer, whose diameter is 30mm and depth is 4.5mm. Thermal paste between the saucer and the hot plate helps limiting the thermal barrier at the interface. The wall temperature of the saucer is measured by a type K thermocouple placed at distance approximately equal to 1mm below the surface, as depicted in Figure 1. This temperature T_w is considered to be a relevant estimation of the saucer wall temperature. When T_w reaches the desired stable value, an urea crystal ball is deposited, which corresponds to the initial time $t=0$. The urea crystals are selected to be 5mg \pm 0.5mg and are manually deposited on the saucer bottom using a wedge clamp. After deposit, the urea crystal ball will evolve differently when T_w is increased, mainly because of chemical reactions. Two high-speed CMOS cameras are used to track this temporal evolution. Camera 1 has a spatial resolution of 896x784 pxl corresponding to approx. 21x18 mm (42.5 pxl/mm). Camera 2 has a spatial resolution of 512x512 pxl corresponding to 14x14 mm (35.6 pxl/mm). Both cameras operate between 1 and 1000Hz, depending on the wall temperature and therefore on the rate of evolution of the urea. The acquisition is stopped after the deposit has reached its final state, i.e. when no more evolution of the deposit is observed.

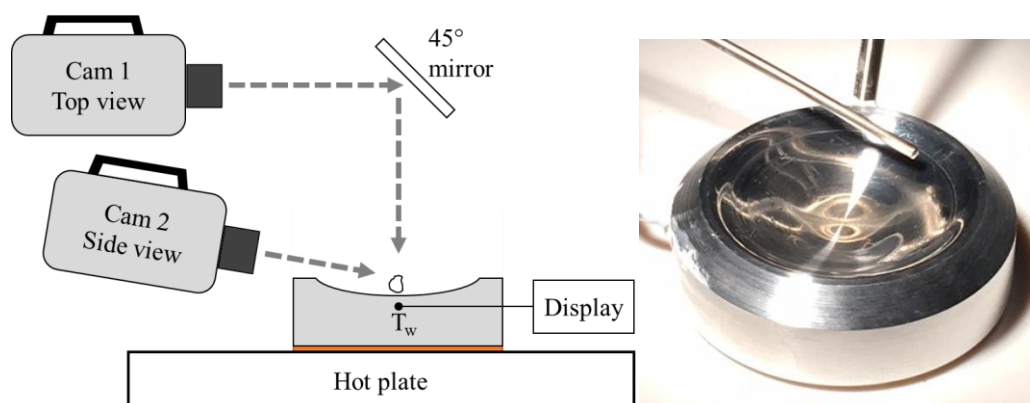


Figure 1 - Schematic representation of the experimental apparatus (left), and picture of the heated saucer.

This experimental setup brings information on two levels. Firstly, it gives access to the delay between the deposit on the saucer bottom surface and the final state. This is linked to the urea thermolysis physics and especially, it can show the apparition a nucleate boiling-like and a Leidenfrost-like regimes, as T_w is increased. Secondly, through the observation of the aspect of the deposit, it also gives insight into the chemical reactions taking place at different wall temperatures.

Computational methodology

In this work, the CONVERGE CFD software package [12] is used as the computational framework for simulating the above experiments of pure urea thermal decomposition on a heated solid surface. CONVERGE is a general purpose CFD code for the calculation of three-dimensional, incompressible or compressible, chemically-reacting fluid flows in complex geometries with stationary or moving boundaries. This code can handle an arbitrary number of species and chemical reactions, as well as transient liquid sprays and films, and laminar or turbulent flows. An innovative modified cut-cell Cartesian method is used that eliminates the need for the computational grid to be morphed with the geometry of interest while still precisely representing the true boundary shape. This approach allows for the use of simple orthogonal grids and completely automates the mesh generation process. Recently, Ebrahimian et al. [1] have proposed a set of coupled models that allows multidimensional simulation of the exhaust system upstream of the SCR monolith [2]. The kinetic mechanism that has been developed is named UWS-12R because it uses a semi-detailed mechanism including 12 reactions (Figure 2). It predicts the formation of ammonia (NH_3) and isocyanic acid (HNCO) upon decomposition of the urea, and the formation of deposits resulting from the polymerization thereof (such as biuret, cyanuric acid and ammeline). According to the authors'

knowledge, these models differ from the previous models in the literature on the two following points: (1) The UWS-12R mechanism considers the competition between thermo-hydrolysis and polymerization in aqueous phase during the UWS temperature growth at the end of water evaporation in the droplets or liquid films. (2) The UWS-12R mechanism models the formation of urea deposits and main polymerization by-products. Our kinetic scheme involves reactions between condensed phase species that have been well documented by Schaber et al. [13]. The resulting kinetic scheme has proved to be a suitable basis for direct coupling with a CFD code [2, 3]. An overview of by-products formation pathways postulated in this mechanism is presented in **Figure 2**. In this study, the different models described in detail in [1, 2] and already implemented in the CONVERGE CFD software package [12] are verified, based on the above experiments.

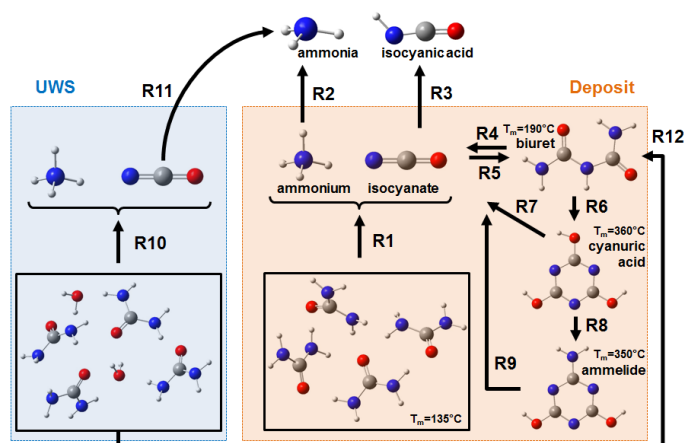


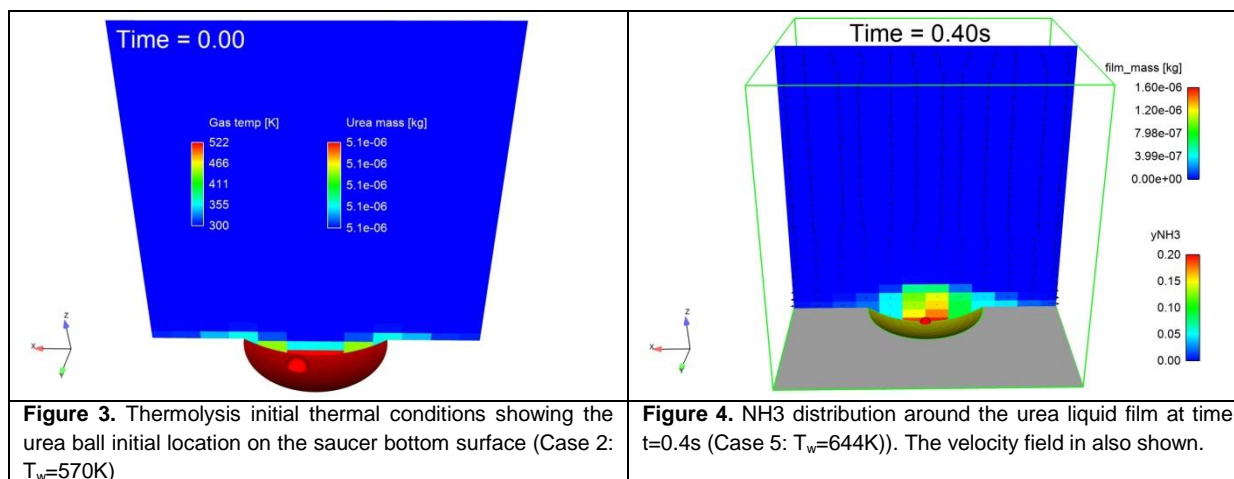
Figure 2. Main reaction pathways (R1) - (R12) to apply for the decomposition of urea in the semi-detailed mechanism UWS-12R. Here only (R1) - (R9) are applied to pure dry urea. The melting temperatures (T_m) of by-products (biuret, cyanuric acid and ammelide) are also shown.

In the above experiments, a rather big solid urea ball ($D_0 \approx 2 \text{ mm}$ and $M_0 \approx 5 \text{ mg}$) is deposited on a heated aluminium plate. Once deposited gently in the saucer, the ball melts and spreads as a liquid film and takes a sessile droplet shape. In this work, we model such sessile droplet as a cylinder with radius r_f and height h_f . In order to compute r_f and h_f , Nagaoka et al. [14] model is used, as described in [15]. A sub-grid liquid film is indeed considered when the obtained area $S_{film} = \pi r_f^2$ is smaller than the wall-cell face area S_w , where the liquid film is located. In this case, the wall heat flux is accounted for only through S_{film} , thereby avoiding its overestimation by using S_w . The SGS liquid film height is also taken equal to h_f as this value is more accurate than the one usually computed as $h_f = \text{Parcels Volume}/S_w$, which value is often underestimated.

In this work, six simulations have been carried out. Five of them are in the third stage of urea thermolysis regimes as described earlier in the above experimental Section. The last simulation (Case 6) uses a wall temperature (T_w) greater than the urea Leidenfrost-like temperature, which have been revealed experimentally in the current work around 650 K. The initial conditions and the physical properties are summarized in **Table 1**. In addition, the melting period has been ignored in the current simulations, as measured experimentally in the third and fourth stages of thermolysis regimes (see next Section). In order to make the simulation thermal conditions close to the experiments at the urea ball deposition, the metallic saucer, whose diameter is 30mm and depth is 4.5mm, has been included in mesh. A relatively coarse grid is used to simplify the liquid film initial condition specification. Indeed, according to the Nagaoka et al. [14] model, the molten urea forms a sessile droplet with diameter $d_f \approx 6 \text{ mm}$, as shown by the image depicted in Figure 6 at low wall temperature. Therefore, $dx=dy=6 \text{ mm}$ have been used in order to ensure the condition: $S_{film} < S_w$ for the SGS liquid film modelling. It is also important to note that using a resolved liquid film with a smaller grid size is possible in the current case. But, the setup of the initial urea liquid film will necessitate several parcels on several wall-faces, as the authors have already performed and validated in [16].

The six simulations are carried out in two steps. First, a simulation is run for two seconds in order to reach thermal equilibrium between the heated saucer and the gas, which was initialized to 300 K, and thereby ensuring the most accurate thermal condition inside the saucer. **Figure 3** shows the thermolysis initial thermal conditions including the urea ball initial location on the saucer surface (Case 2: $T_w=570 \text{ K}$) in the beginning of the second step simulation. **Figure 4** presents an example of the NH_3 distribution around the urea liquid film in the central cut-plane at time $t=0.4 \text{ s}$ for Case 5. The non-symmetric NH_3 cloud is due to initial position of the liquid film (**Figure 3**) and the velocity field also shown in **Figure 4**.

In **Table 1** are also summarized the different gas temperature at the bottom of the saucer (T_{Saucer}) obtained by the first step simulations. Finally, typical time-step used in these simulations is 10^{-3} s.



Case #	Units	1	2	3	4	5	6
Wall temperature (T_w)	[K]	540	570	595	619	644	669
Urea ball mass (M_0)	[mg]	5.3	5.1	4.9	4.5	4.8	5.2
Gas T_{Saucer}	[K]	495	522	543	563	585	607
Viscosity	[N*s/m ²]	1.01E-04	9.10E-05	8.21E-05	8.02E-05	8.02E-05	8.02E-05
Surf tension	[N/m]	2.21E-02	1.50E-02	9.43E-03	3.76E-03	0.81E-03	0.35E-03
Conductivity	[W/(m*K)]	2.85E-01	2.76E-01	2.68E-01	2.60E-01	2.51E-01	2.44E-01
Density	[kg/m ³]	1.28E+03	1.28E+03	1.28E+03	1.28E+03	1.28E+03	1.28E+03
Specific heat	[J/(kg*K)]	1.50E+03	1.50E+03	1.50E+03	1.50E+03	1.50E+03	1.50E+03

Results and discussion

The experimental and numerical results as a function of wall temperature T_w are presented in Figure 5 concerning the evolution time (i.e. the time needed to reach the final state), and in Figure 6 concerning the evaporation regimes and final products. T_w was varied between 406K and 716K for the experiments, and between 540K and 669K for the simulations. Additionally, the numerical results in terms of urea and by-products (biuret, cyanuric acid (CYA) and ammelide) mass are depicted in **Figure 7** and **Figure 8**.

The first analysis consists in measuring the time needed to reach the final state (also referred to below as evolution time or t_{evol}), as a function of the wall temperature. The results are presented in Figure 5, for 2 repetitions of the experiment, and for 2 parametrisations of the simulation (black curves). For wall temperatures below 460K, the evolution time corresponds to the fusion of urea only. Indeed, no visible chemical reactions (or bubbles) appear for $T_w < 460\text{K}$. At $T_w > 460\text{K}$, the evolution time corresponds to fusion and urea decomposition, explaining the sudden increase of t_{evol} around 460K. Figure 5 also shows that the evolution time reaches a minimum value of less than 1s between approx. 620K and 650K. This behaviour is similar to what has previously been observed for single component liquids [8, 11] or urea-water solutions [17]. On the simulation results, since the ammelide mass reaches a quasi-constant value for Case 1 to Case 5, the numerical evolution time t_{evol} has been sought out based on the ammelide production rate defined as $\varepsilon = \text{Ammelide mass production rate}/M_0$, where M_0 is the initial urea mass. The numerical evolution time has been defined from **Figure 8** as the time when the ammelide production rate is smaller than a specified value, denoted $\varepsilon_{\text{evol}}$. Two values for $\varepsilon_{\text{evol}}$ have been tested, $2 \cdot 10^{-3}$ and $4 \cdot 10^{-3}$. For cases 1 to 5, both CYA and ammelide reach a quasi-constant mass, as shown in **Figure 7**. This is not the case for Case 6 ($T_w=669\text{K}$), therefore no evolution time is computed, neither numerically nor experimentally because of the observed violent thermal breakup expelling the urea droplet outside of the camera's fields. For both values of $\varepsilon_{\text{evol}}$, the numerical results are in very good agreement with the experimental results, as shown in the zoom of Figure 5. This means that the UWS-12R thermolysis mechanism depicted in **Figure 2** is able to follow the strong variation of the evolution time when increasing the wall temperature for cases 1 to 5.

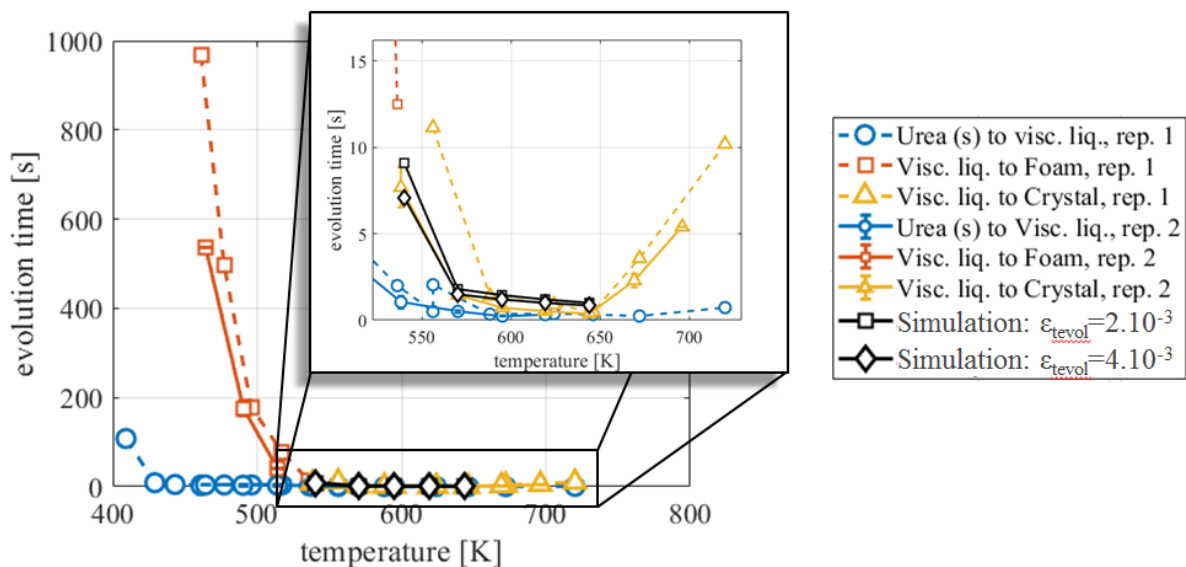


Figure 5. Effect of wall temperature on the evolution time of the deposit.

The evolution of the deposit is also analysed between the initial and the final state, using the same terminology as in [8, 10, 11].

For wall temperatures between 460K and 630K, the experimental results show that some gas bubbles appear inside the deposit, which is thus in nucleate boiling-like regime. The final products appear to be a white foam that tends to turn into a white crystal for $T_w > 540\text{K}$, as described in Figure 6. Interestingly, although wall temperature is above the biuret fusion temperature (463K), the final products seem to be completely under solid form. So, it can be assumed that the observed final deposit is a mixture of by-products heavier than biuret, such as CYA and ammelide. This is confirmed by the numerical results as shown in **Figure 7**. As can be seen in this Figure, biuret is always formed first, followed by CYA. Then, ammelide production starts at the biuret thermolysis end, which lifetime is short. It is important to note that only the heaviest by-products (CYA and ammelide) are always present at the end of the simulation, whatever is the wall temperature. Ammelide is formed from CYA as depicted in the semi-detailed thermolysis mechanism UWS-12R (**Figure 2**).

For wall temperatures between 630K and 650K, the experimental results show that the evolution seems to be in a transition regime. The final products seem to slightly change colour, becoming a brownish crystal. This can be an indication that the final product contains more and more ammelide, as shown by the numerical results in **Figure 7**. But, it can also be an indication that other species (like Ammeline and melamine) are formed, although not specifically modelled in the CFD code. Indeed, UWS-12R mechanism assumes that ammelide represents all urea by-products heavier than CYA.

At last, for wall temperatures above approx. 650K, a clear Leidenfrost-like regime is revealed experimentally. This behaviour is similar to what has previously been observed for single component liquids [8, 11] or urea-water solutions [17]. In those UWS cases, the film boiling regime is created by the evaporation of the liquid film [15]. In the case of the urea crystal, though there is almost no urea evaporation phenomenon, this Leidenfrost regime also appears, but is governed by urea gasification into ammonia (NH_3) and isocyanic acid (HNCO). It must be noted that, because of the Leidenfrost-like regime, the evolution time shown in Figure 5 is difficult to identify because the levitating droplet suffers from explosions leading to the formation of several smaller droplets, some of them exiting the field of view. In the CFD code, a Leidenfrost-like behaviour is therefore considered for $T_w > 650\text{K}$ using the same Leidenfrost model as for hydrocarbons. More details about the Leidenfrost model may be found in Habchi et al. [16]. During the levitation of the urea droplet in Case 6, urea thermolysis evolution is similar to urea liquid films in the third thermolysis regime. However, because of higher T_w in this case, CYA and ammelide does not reach a quasi-constant mass (see **Figure 7**), and their values are decreasing as they are decomposed in their turn to NH_3 and HNCO . Noteworthy, the much higher time ($>100\text{ s}$) that urea thermolysis takes in the Leidenfrost-like Case 6.

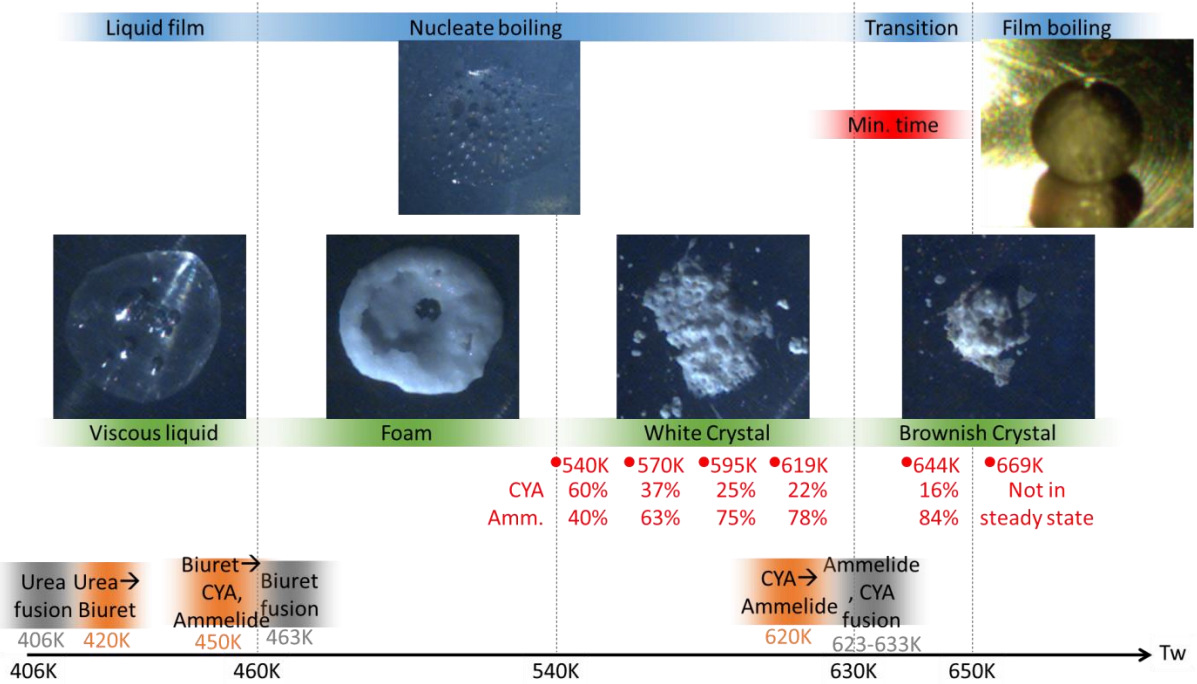


Figure 6. Summary of the observed phenomena. Blue: Evolution regime. Green appearance of the final product. Gray and orange: Characteristic temperatures. The red circles symbolize the simulated wall temperatures, and the corresponding residual composition at the end of evolution.

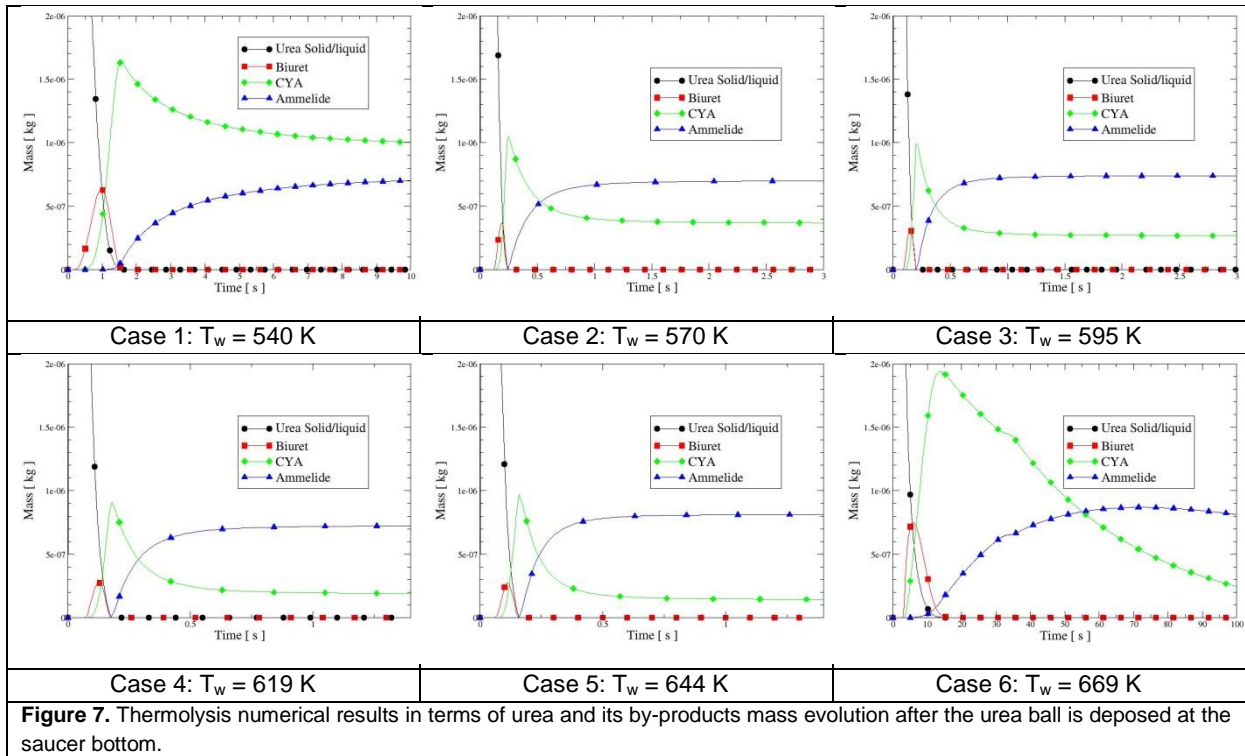


Figure 7. Thermolysis numerical results in terms of urea and its by-products mass evolution after the urea ball is deposited at the saucer bottom.

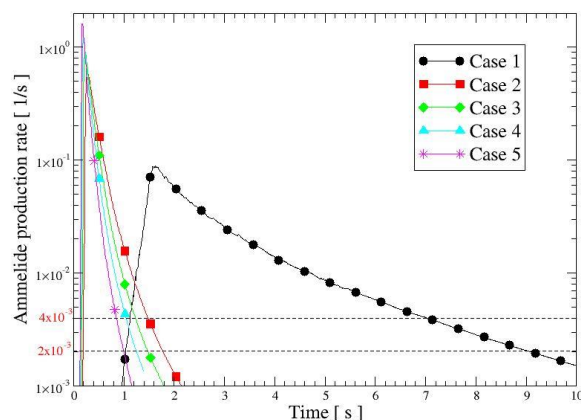


Figure 8. Numerical results in terms of ammelide production rate (ϵ). The dashed lines at $\epsilon_{tevol}=2 \times 10^{-3}$ and $\epsilon_{tevol}=4 \times 10^{-3}$ correspond to the range in which the time (t_{evol}) to reach a solid deposit is observed experimentally. **Table 2** summarizes the experimental and numerical (t_{evol}) results.

Case #	1	2	3	4	5
Wall temperature [K]	540	570	595	619	644
(t_{evol}) experiments [s]	8.3 ± 1.7	1.85 ± 0.5	0.95 ± 0.5	0.55 ± 0.5	0.55 ± 0.3
(t_{evol}) Simulations [s] with $\epsilon_{tevol} = 10^{-8}$	9.1	1.8	1.45	1.2	1.0
(t_{evol}) Simulations [s] with $\epsilon_{tevol} = 2.10^{-8}$	7.1	1.5	1.2	1.0	0.85

Conclusions

In this work, the behaviour of solid/liquid urea after being deposited on a heated surface have been investigated experimentally and numerically..

The experiments have revealed the existence of a Leidenfrost-like temperature for urea at around 650K. Contrary to standard Leidenfrost regimes governed by the evaporation of the liquid film, the Leidenfrost-like regime of solid urea is controlled by the different thermolysis reactions producing gaseous NH_3 and $HNCO$. This Leidenfrost-like regime is modelled in the CFD code which has been demonstrated very useful for the accuracy of wall/urea interaction in CFD modelling of SCR systems. In addition, the numerical and experimental results compare quite well in terms of the time needed to reach a final state, which shows the good behaviour of the recently developed UWS-12R thermolysis mechanism when the thermal conditions are properly simulated. Additional experiments where the composition of the final products is analysed would be required to further validated the UWS-12R mechanism.

Acknowledgements

The authors would like to acknowledge Virgile Straub and Clément Bramoullé from IFPEN who performed the experiments.

References

- [1] Ebrahimian, V., Nicolle, A., and Habchi, C., "Detailed modeling of the evaporation and thermal decomposition of urea-water solution in SCR systems," *AICHE JOURNAL* 58(7):1998–2009, 2012, doi:10.1002/aic.12736.
- [2] Habchi, C and Nicolle, A and Gillet, N, "Numerical-Study-of-Deposits-Formation-in-SCR-Systems-Using-Urea-Water-Solution-Injection," *J Mater Sci Nanotechnol* 6(2), 2018.

- [3] Habchi, C., Quan, S., Drennan, S., and Bohbot, J. (eds.), "Towards Quantitative Prediction of Urea Thermo-Hydrolysis and Deposits Formation in Exhaust Selective Catalytic Reduction (SCR) Systems," SAE Technical Paper N° 2019-01-0992, 2019.
- [4] Lauer, T., "Preparation of Ammonia from Liquid AdBlue - Modeling Approaches and Future Challenges," *Chemie Ingenieur Technik* 90(6):783–794, 2018, doi:[10.1002/cite.201700107](https://doi.org/10.1002/cite.201700107).
- [5] Brack, W., Heine, B., Birkhold, F., Kruse, M. et al., "Formation of Urea-Based Deposits in an Exhaust System: Numerical Predictions and Experimental Observations on a Hot Gas Test Bench," *Emiss. Control Sci. Technol.* 2(3):115–123, 2016, doi:[10.1007/s40825-016-0042-2](https://doi.org/10.1007/s40825-016-0042-2).
- [6] Sun, Y., Sharma, S., Vernham, B., Shibata, K. et al., "Urea Deposit Predictions on a Practical Mid/Heavy Duty Vehicle After-Treatment System," *SAE Technical Paper NO. 2018-01-0960*, doi:[10.4271/2018-01-0960](https://doi.org/10.4271/2018-01-0960).
- [7] Quan, S., Wang, M., Drennan, S., Strodbeck, J. et al., "A Molten Solid Approach for Simulating Urea-Water Solution Droplet Depletion: in: ILASS Americas, 27th Annual Conference on Liquid Atomization and Spray Systems, Raleigh, NC, May 2015."
- [8] Xiong, T.Y. and Yuen, M.C., "Evaporation of a liquid droplet on a hot plate," *International Journal of Heat and Mass Transfer* 34(7):1881–1894, 1991, doi:[10.1016/0017-9310\(91\)90162-8](https://doi.org/10.1016/0017-9310(91)90162-8).
- [9] Stanglmaier, R.H., Roberts, C.E., and Moses, C.A., "Vaporization of Individual Fuel Drops on a Heated Surface: A Study of Fuel-Wall Interactions within Direct-Injected Gasoline (DIG) Engines," *SAE Technical Paper NO. 2002-01-0838*, doi:[10.4271/2002-01-0838](https://doi.org/10.4271/2002-01-0838).
- [10] Moita, A.S. and Moreira, A.L.N., "Drop impacts onto cold and heated rigid surfaces: Morphological comparisons, disintegration limits and secondary atomization," *International Journal of Heat and Fluid Flow* 28(4):735–752, 2007, doi:[10.1016/j.ijheatfluidflow.2006.10.004](https://doi.org/10.1016/j.ijheatfluidflow.2006.10.004).
- [11] Bernardin, J.D. and Mudawar, I., "The leidenfrost point: Experimental study and assessment of existing models," *Journal of Heat Transfer* 121(4):894–903, 1999, doi:[10.1115/1.2826080](https://doi.org/10.1115/1.2826080).
- [12] Richards K. J., Senecal P. K., Pomraning E., CONVERGE: CONVERGECFD MANUAL SERIES (2.4), Convergent Science, Madison, WI, <https://convergecf.com/>, 2018.
- [13] Schaber, P.M., Colson, J., Higgins, S., Thielen, D. et al., "Thermal decomposition (pyrolysis) of urea in an open reaction vessel," *Thermochimica Acta* 424(1-2):131–142, 2004, doi:[10.1016/j.tca.2004.05.018](https://doi.org/10.1016/j.tca.2004.05.018).
- [14] Nagaoka, M., Kawazoe, H., and Nomura, N. (eds.), "Modeling Fuel Spray Impingement on a Hot Wall for Gasoline Engines: SAE Technical paper 940525," SAE, 1994.
- [15] Habchi, C., "A Comprehensive Model for Liquid Film Boiling in Internal Combustion Engines," *Oil & Gas Science and Technology - Rev. IFP Energies nouvelles* 65(2):331–343, 2010, doi:[10.2516/ogst/2009062](https://doi.org/10.2516/ogst/2009062).
- [16] Habchi, C., Lamarque, N., Helie, J., and Jay, S., "Experimental and Numerical Investigation of Dispersed and Continuous Liquid Film under Boiling conditions," *Proceedings ILASS–Europe 2017. 28th Conference on Liquid Atomization and Spray Systems*, ILASS2017 - 28th European Conference on Liquid Atomization and Spray Systems, 6/9/2017 - 8/9/2017, Universitat Politècnica València, Valencia, ISBN 9788490485804, 2017.
- [17] Musa, S.N.A., Saito, M., Furuhashi, T., and Arai, M. (eds.), "Evaporation characteristics of a single aqueous urea solution droplet," 10th International Conference on Liquid Atomization and Spray Systems, ICLASS 2006, 2006.